# Modeling Enzyme–Inhibitor Interactions in Serine Proteases

**MARIA JOÃO RAMOS,[1] ANDRÉ MELO,[1] ELSA S. HENRIQUES,[1] JOSÉ A. N. F. GOMES,[1] NATHALIE REUTER,[2] BERNARD MAIGRET,[2] WELY B. FLORIANO,[3] MARCO A. C. NASCIMENTO[4]**

[1] CEQUP/Departamento de Química, Faculdade de Ciências, Universidade do Porto, Rua do Campo Alegre 687, 4150 Porto, Portugal
[2] Laboratoire de Chimie Théorique, UA CNRS 510, Université Henri Poincaré, Nancy-I B.P. 239, 54506 Vandoeuvre-les-Nancy Cedex, France
[3] Centro de Ciências Exatas, Departamento de Física, Universidade Federal do Espírito Santo, Vitória, ES, 29060-900, Brazil
[4] Departamento de Físico-Química, Instituto de Química, Universidade Federal do Rio de Janeiro, Rio de Janeiro, RJ, 21949-900, Brazil

**ABSTRACT:** We are interested in modeling enzyme–inhibitor interactions with a view to improve the understanding of the biology of these processes. The present work focuses, therefore, on the research on enzyme–inhibitor interactions using two highly homologous enzymes as our models: $\beta$-factor XIIa and trypsin. This study so far has focused on the following: (1) arginine–carboxylate interactions such as the one occurring in the "binding pocket" of $\beta$-factor XIIa with an inhibitor; according to the present calculations, the neutral form is usually more stable than is the zwitterion in hydrophobic environments as in the case of the above-mentioned complex. (2) Interactions present in the contact region between trypsin and PTI; the contribution of some amino acids of that region to the binding energy of the complex trypsin–PTI was determined using free-energy simulation methods. (3) Interactions involved in the inhibition of trypsin by PTI; hybrid quantum-classical mechanical calculations (LSCF) were performed to further this point.   © 1999 John Wiley & Sons, Inc. Int J Quant Chem 74: 299–314, 1999

**Key words:** quantum methods; free energy; LSCF; trypsin, $\beta$-factor XIIa

## Introduction

**M**olecular modeling is a new exciting field, a rapidly growing area contributing to increased knowledge on molecular structure, function, and interaction. Everyday, attempts are being made in studying larger and more complex systems, increasing the number of publications available in the literature on the subject and helping out the experimentalists with the interpretation of experiments and/or the design of new ones.

We are interested in modeling enzyme–inhibitor interactions with a view to improving the understanding of the biology of these processes. Systems of particular interest to us are serine proteases, namely, $\beta$-factor XIIa and trypsin, and their respective inhibitors. Those enzymes are both of great biological importance: $\beta$-Factor XIIa belongs to the group of blood coagulation proteins and trypsin is a pancreatic serine protease involved in digestion.

The enzymes show sequence identity to a high degree, and although the physiological functions of the two proteins are different, they seem to have the same active center (formed by the catalytic triad Ser 195, His 57, and Asp 102) [1, 2] and to follow the same catalytic mechanism. However, the pancreatic trypsin inhibitor (PTI), which is a natural inhibitor of trypsin, does not inhibit $\beta$-factor XIIa; moreover, the amazing stability of the complex formed between trypsin and PTI [3] has not really been explained. What is the contribution of each residue to the binding energy? The conformation of this complex is often used, in reactivity studies, as a model of the Michaelis complex which generally leads to the formation of the acyl enzyme and then to the hydrolysis of PTI. However, why is there no hydrolysis of PTI? Why is there no cleavage of the peptidic bond of PTI considering the great similarity between this inhibitor and a substrate for trypsin?

These are the sort of questions that we are attempting to answer. The present work so far has focused on the study of the following:

1. *Interactions occurring in the ''binding pocket'' of $\beta$-factor XIIa with an inhibitor*, that is, salt bridge electrostatic interactions formed between the aspartate which sits at the end of the binding pocket of $\beta$-factor XIIa and the arginine characteristic of any inhibitor or indeed any $\beta$-factor XIIa substrate preferred by the enzyme. We performed ab initio (6-31G** and MP2/6-31G**) [4] and semiempirical (AM1) [5] calculations for this study.

2. *Interactions occurring in the contact region between trypsin and PTI*, that is, calculations on the change in the binding free energy associated with mutations carried out in trypsin when within the complex trypsin–PTI, using free-energy simulation methods [6], to understand the contribution of each amino acid to the binding energy of the complex.

3. *Interactions involved in the inhibition of trypsin by PTI*, by hybrid quantum-classical mechanical calculations (LSCF) [7] on the complex trypsin–PTI combining a quantum treatment of the catalytic site of the enzyme and the part of the inhibitor in close contact with it, and a classical treatment of the rest of the system. The objective of these studies is to find out why PTI behaves as an inhibitor of trypsin rather than as a substrate.

## Interactions Occurring in the ''Binding Pocket'' of $\beta$-Factor XIIa with an Inhibitor

There has been much interest focused on the interactions between acidic amino acids, aspartic (Asp) and glutamic (Glu), and arginine (Arg). Indeed, these side-chain interactions are very important, amounting to 40% of ionic pairs occurring in proteins [8, 9]. They have been usually viewed as guanidinium–carboxylate salt bridges as these ions are the terminus of the Arg side chain and the Asp and Glu side chains, respectively. However, the interactions Arg–Asp and Arg–Glu (arginine–carboxylate interactions) can occur in two different forms: zwitterionic and neutral. These forms can be well simulated using appropriate molecular models such as methylguanidinium–acetate and methylguanidine–acetic acid, respectively (see Fig. 1).

The arginine–carboxylate interactions undertake a very important role in a large number of biological mechanisms such as in the photochemistry of retinal protein [10–14], antigen/antibody recognition [15–17], and enzyme–substrate interactions [18, 19] (in which $\beta$-factor XIIa–inhibitor interactions are included [20]).
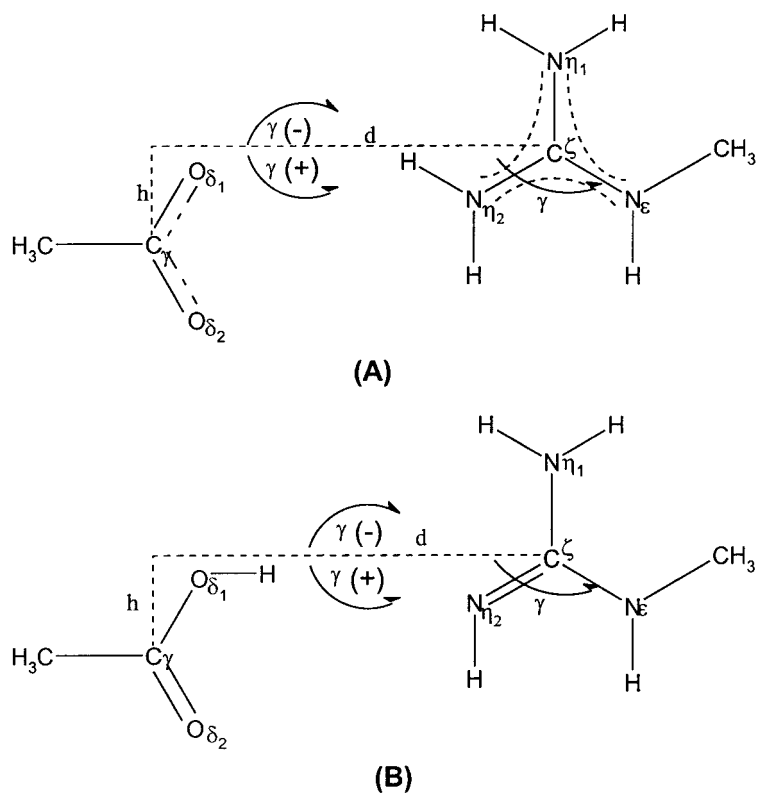
**FIGURE 1.** Schematic representation of (A) methylguanidinium−acetate and (B) methylguanidine−acetic acid. In both systems, the intermolecular parameters $\gamma$, $h$, and $d$ are also shown.

The interest in these interactions has been translated into a series of studies, which can be found in the literature [9, 21−26]. Both experimental, that is, systematic analysis of structural crystallographic data, and the theoretical work, performed on a very restricted set of configurations and at a low quantum mechanical level, have favored the zwitterionic form.

In this context, some of us have performed extensive quantum-mechanical studies of this system [7, 27−29]. In these studies, we carried out semiempirical AM1 calculations, as well as using LSCF and ab initio (6-31G** and MP2/6-31G**) methods. According to these calculations, the neutral form is usually more stable than is the zwitterion in hydrophobic environments (such as the binding pocket of $\beta$-factor XIIa) [7, 27−29]. On the other hand, the interactions with a hydrophilic proteic or aqueous environment stabilize the zwitterionic form relatively to the neutral one [7].

The large influence of the environment on the arginine−carboxylate binding processes has also been confirmed by other recent theoretical studies

[30−32]. It is concluded that, in general, in the folding of proteins, the formation of salt bridges is not favored and the ion-pair structure is preferred over the neutral species. However, this situation seems to be inverted in some hydrophobic environments [30].

The analysis of our energetic and structural results also enabled us to conclude that the electronic correlation does not introduce any significant enhancement to the values calculated at the 6-31G** level [28]. On the other hand, the AM1 results exhibit large differences when compared with the ab initio values [28]. However, only symmetric conformations ($h = 0$) were considered in our conformational studies (see Fig. 1). The staggered conformations ($h \neq 0$), of which some are very important, were ignored.

In this work, a conformational analysis was carried out *in vacuo* on both forms: zwitterionic and neutral. This study was performed using the ab initio RHF method with a 6-31G** basis set [4], because this seems to be the lower quantum-mechanical level that gives a good description of argi-

nine–carboxylate interactions [28]. All the calculations were done within the package GAUSSIAN 92 [33], using an IBM Risc 6000 workstation.

Most arginine–carboxylate interactions seem to occur when the heavy atoms of both fragments are on the same plane [9, 23]. We, thus, limited our study to this region; Figure 1 shows the intermolecular parameters that have been used to create the conformational space, that is, $\gamma$, $d$ and $h$. After fixing the rotation angle $\gamma$ of one molecule against the other, we optimized the other intermolecular parameters, that is, the distances $d$ and $h$ between the carbon atoms $C_\gamma$ and $C^\zeta$ of both molecules, as well as the inherent intramolecular parameters.

$Trans$(H), corresponding to $\gamma = 60°$, and $trans$(CH$_3$), with $\gamma = 180°$, were the starting geometries for the conformational analysis, with each conformation having been obtained from the previous optimized one with an increment in $\gamma$ of 10°. This led us to 36 studied conformations for each form, that is, 72 conformations in total.

The stabilization energy ($\Delta E$) for our systems was also calculated here using the supermolecule approach and the noninteracting charged fragments as the initial reference state:

$$\Delta E = E(S) - E(MGH^+) - E(Ac^-), \quad (1)$$

with $E(S)$ standing for the energy of the neutral (MG:HAc) or zwitterionic (MGH$^+$:Ac$^-$) forms; $E(MGH^+)$, the energy of the methylguanidinium; and $E(Ac^-)$, the energy of the acetate ion. The counterpoise correction was not used in these calculations, because it has been determined to be very small in this type of system [28].

Figure 2 depicts the results that we have obtained with the present conformational analysis and help us to conclude that the neutral form is, indeed, usually more stable than is the zwitterion. There are exceptions occurring at $\gamma = -50°$ to $-10°$ in which the only protons being transferred are those from the methyl group of methylguanidinium. The minima of conformational space occur with conformations $trans$(H), with $\gamma = 60°$, and $trans$(CH$_3$), with $\gamma = 180°$; this is in agreement with both the analysis of the structural data [9, 21, 23] and the theoretical calculations [23–29] previously done.

Previously [27, 28], proton transfer had been detected occurring from methylguanidinium to the acetate during the ab initio optimization procedure. However, this phenomenon was observed in a very small number of conformations. Here, due to the possibility of horizontal displacements during the optimization procedure, the path for proton transfer is more realistic and easier. Therefore,
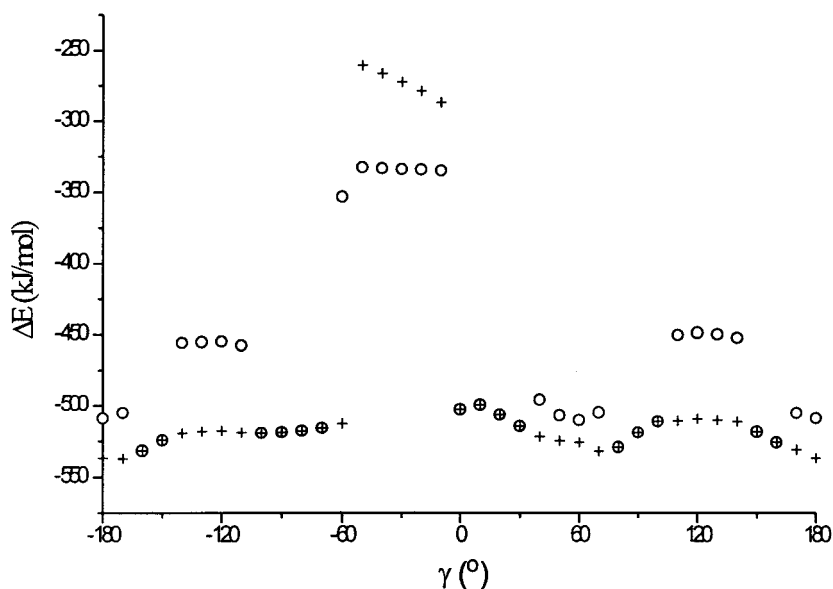


**FIGURE 2.** Plot of stabilization energy $\Delta E$(kJ/mol) versus angle of rotation $\gamma$ (degree) for ($\bigcirc$) methylguanidinium against acetate, (+) methylguanidine versus acetic acid, and ($\oplus$) conformations where proton transfer has been observed during the optimization procedure from a zwitterionic initial geometry.

proton transfer has been observed in a very large number of conformations ($-160°$, $-150°$, $-100°$, $-90°$, $-80°$, $-70°$, $0°$, $10°$, $20°$, $30°$, $80°$, $90°$, $100°$, $150°$, and $160°$).

Crystallographic data cannot usually provide information on the position of hydrogen atoms and, so, a complete description of arginine–carboxylate interactions may fail if we restrict these atoms to the amino acid side chains to which they would normally belong. The evidence of a proton transfer occurrence in arginine–carboxylate complexes can be indirectly detected by the *break of symmetry* in the heavy atom geometric parameters induced in the respective side chains [34]. However, this possibility has to be explicitly taken into account in the refinement procedures of crystallographic structures [34].

In this work, we carried out a statistical study on these relevant geometric parameters for all the fragments studied (acetate, acetic acid, methylguanidinium, and methylguanidine), both isolated and when included in the zwitterionic or neutral complexes. The geometric parameters were defined using standard orientations of the fragments in relation to the more closely interacting oxygen for acetate in presence of methylguanidinium, the proton-acceptor oxygen in acetic acid, the methyl group for isolated methylguanidinium, the removed proton for isolated methylguanidine, the transferred proton for methylguanidine in the presence of acetic acid, and the more closely interacting hydrogen for methylguanidinium in the presence of acetate (see Fig. 3).

For fragments in each other's presence, the mean values of the geometric parameters are obtained as conformational averages. All the structures used in this study were optimized with the already referred to constraints. No type of weighting factor was used because our main objective was to test the conformational invariance of the standard orientations. For isolated methylguanidine, these values are obtained as averages for all possible structures (differing in which proton has been removed). For the other isolated fragments (methylguanidinium, acetate, and acetic acid), only one structure occurs and the geometrical parameters are unambiguously defined. The results obtained in this study are presented in Table I.

The carboxylate group of isolated acetate is a $\pi$-conjugated system where the two $C\text{:::}O$ ($d_1$ and $d_2$) bonds and $CH_3\text{—}C\text{:::}O$ ($a_1$ and $a_2$) angles are equivalent. In isolated acetic acid, this symmetry is broken by the proton transferred to
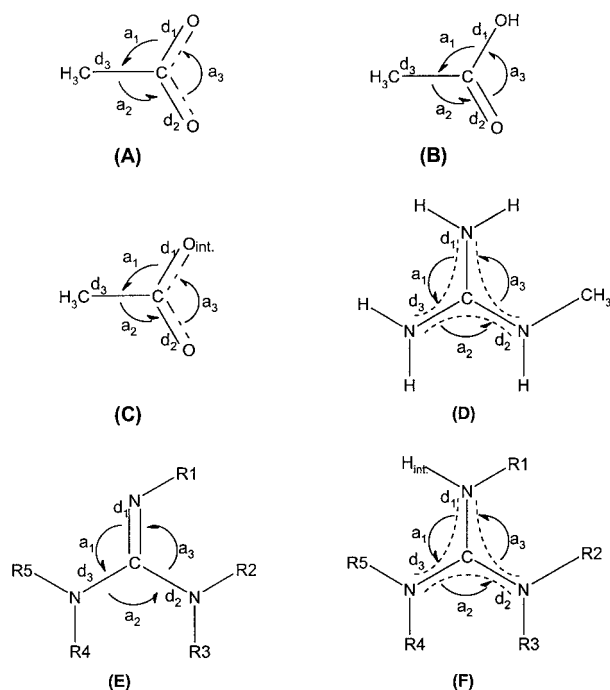


**FIGURE 3.** Standard orientations used in the statistical analysis of heavy atom geometric parameters ($d_1$, $d_2$, $d_3$, $a_1$, $a_2$, and $a_3$) associated with proton transfer for (A) isolated acetate, (B) acetic acid, (C) acetate in presence of methylguanidinium, (D) isolated methylguanidinium, (E) methylguanidine, and (F) methylguanidinium in presence of acetate. In the ionic fragments (C and F); $H_{int}$ represents the hydrogen atom of methylguanidinium which more closely interacts with acetate and $O_{int}$ represents the oxygen atom of acetate which more closely interacts with methylguanidinium, respectively.

an oxygen atom originating one single $C\text{—}OH$ ($d_1$) and one double $C=O$ ($d_2$) localized bond. Consequently, $d_1$ increases (from 1.24 to 1.33 Å) and $d_2$ decreases (from 1.24 to 1.19 Å). The associated angles $CH_3\text{—}C\text{—}OH$ ($a_1$) and $CH_3\text{—}C\text{:::}O$ ($a_2$) also become nonequivalent. Therefore, while $a_1$ decreases from $115.25°$ to $111.95°$, $a_2$ increases from $115.25°$ to $125.71°$. The remaining angle $O=C\text{—}O$ ($a_3$) and bond $C\text{—}CH_3$ ($d_3$) change from $129.50°$ to $122.34°$ and from 1.55 to 1.50 Å, respectively.

The isolated methylguanidinium is also a $\pi$-conjugated system where the three $C\text{:::}N$ ($d_1$, $d_2$, and $d_3$) bonds and $N\text{:::}C\text{:::}N$ ($a_1$, $a_2$, and $a_3$) angles are almost equivalent. In the isolated methylguanidine, this quasi-symmetry is broken by the proton removed from a nitrogen atom. This originates two single $C\text{—}N$ ($d_2$ and $d_3$) bonds and one double $C=N$ ($d_1$) localized bond. Consequently,

**TABLE I**

Geometric parameters[a,b] average of heavy atoms and co-standard deviations[c] associated with proton transfer.

| Fragment | $d_1$ | $d_2$ | $d_3$ | $a_1$ | $a_2$ | $a_3$ |
|---|---|---|---|---|---|---|
| Isolated Ac$^-$ | 1.24 | 1.24 | 1.55 | 115.25 | 115.25 | 129.50 |
| Isolated HAc | 1.33 | 1.19 | 1.50 | 111.95 | 125.71 | 122.34 |
| Ac$^-$ in presence of MGH$^+$ | $1.2 \pm 0.8$ | $1.2 \pm 0.5$ | $1.5 \pm 0.1$ | $116 \pm 2$ | $118 \pm 2$ | $126.1 \pm 0.6$ |
| HAc in presence of MG | $1.3 \pm 0.5$ | $1.2 \pm 0.3$ | $1.5 \pm 0.9$ | $112 \pm 1$ | $124 \pm 1$ | $124.1 \pm 0.2$ |
| Isolated MGH$^+$ | 1.32 | 1.32 | 1.33 | 119.28 | 120.06 | 120.66 |
| Isolated MG | $1.26 \pm 0.01$ | $1.38 \pm 0.01$ | $1.38 \pm 0.01$ | $120.2 \pm 0.7$ | $112 \pm 1$ | $127.0 \pm 0.7$ |
| MGH$^+$ in presence of Ac$^-$ | $1.30 \pm 0.01$ | $1.34 \pm 0.01$ | $1.33 \pm 0.01$ | $120.4 \pm 0.9$ | $119 \pm 1$ | $120.9 \pm 0.9$ |
| MG in presence of HAc | $1.27 \pm 0.01$ | $1.38 \pm 0.01$ | $1.37 \pm 0.01$ | $120.6 \pm 0.7$ | $114 \pm 1$ | $125 \pm 1$ |

Ac$^-$—acetate; HAc—acetic acid; MGH$^+$—methylguanidinium; MG—methylguanidine.
[a] Bond lengths in angstroms, angles in degrees.
[b] The geometric parameters are defined according to the standard orientation presented in Figure 3.
[c] Standard deviations calculated relatively to the average structures.

while $d_1$ decreases from 1.32 to 1.26 Å, $d_2$ and $d_3$ both increase to 1.38 Å. This quasi-symmetry is also broken relatively to the bond angles. In fact, while $a_1$ is almost conserved at 120°, $a_2$ changes from 120.06° to 112°, and $a_3$, from 120.60° to 127.0°.

When the fragments are included in the respective complexes, the above-mentioned tendencies are usually observed. However, the fragment–fragment interactions led to less marked differences between the ionic and neutral species.

Our present results are in good agreement with our previous theoretical calculations [7, 27–29], the latter strongly suggesting that in hydrophobic environments the neutral form should be more stable than is the zwitterionic one. Here, the improvement of the molecular model reinforced the previous conclusions. Additionally, we used a methodology, based in the *break of symmetry* induced by proton transfer in some heavy atom geometric parameters [34], to detect the occurrence of the neutral arginine–carboxylate complex in crystallographic structures.

## Interactions Occurring in the Contact Region Between Trypsin and PTI

Enzymes control most biochemical reactions occurring in living organisms. The best way to investigate the catalytic mechanisms of these biopolymers would be to crystallize the enzyme:substrate complexes and examine their structures by X-ray diffraction or NMR techniques. Unfortunately, a complex of this type is very unstable, and once it is formed, the catalytic reaction begins rapidly originating the corresponding enzyme–product complex [1].

We are interested in serine protease inhibitors of the PTI type, and throughout the text when mentioning inhibitors, we are referring to such systems. Naturally occurring serine protease inhibitors of the PTI type are usually small proteins which undertake an important biological role in the control and defense mechanisms of living organisms. The inhibitors bind reversibly to enzymes in a similar manner as substrates do. However, an enzyme–inhibitor structure is stabilized by a complex system of noncovalent (hydrogen bond, van der Waals, and electrostatic) interactions which inactivate the enzyme blocking its active site.
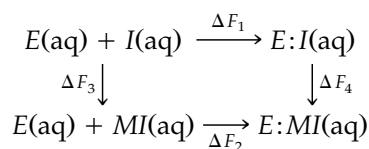
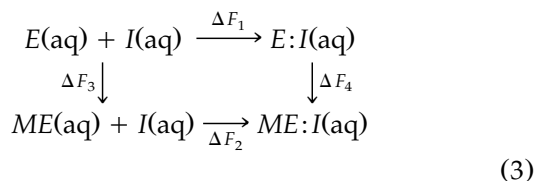In this context, the simulation of enzyme ($E$)–inhibitor ($I$) association reactions,

$$E(\text{aq}) + I(\text{aq}) \rightarrow E{:}I(\text{aq}), \qquad (2)$$

is very important to model the corresponding enzyme–substrate association processes. These theo-

retical studies contribute to a better understanding of the interactions responsible for the stability of enzyme−inhibitor complexes, and this knowledge should be very important in the design of new specific inhibitors.

Presently, simulation of the association reactions (2) is usually impossible, mainly because it would mean removing a large number of water molecules from the solvated enzyme and inhibitor to form the enzyme−inhibitor complex. However, it is possible to perform this type of study using indirect pathways. The most used methodology consists of performing relevant amino acid mutations selected in the contact region of the enzyme: inhibitor complex, creating a modified enzyme (ME) or inhibitor (MI). A mutation of this type should destroy the specificity of a given interaction, preserving the three-dimensional structure of the original species. Consequently, the original and mutated residues should be similar from a topological point of view but must have different chemical properties. In this context, the binding free energy ($\Delta\Delta F$), associated with a particular mutation, can be determined using appropriate thermodynamic cycles,

$$\begin{array}{ccc} E(\text{aq}) + I(\text{aq}) & \xrightarrow{\Delta F_1} & E{:}I(\text{aq}) \\ \Delta F_3 \downarrow & & \downarrow \Delta F_4 \\ ME(\text{aq}) + I(\text{aq}) & \xrightarrow{\Delta F_2} & ME{:}I(\text{aq}) \end{array}$$

or (3)

$$\begin{array}{ccc} E(\text{aq}) + I(\text{aq}) & \xrightarrow{\Delta F_1} & E{:}I(\text{aq}) \\ \Delta F_3 \downarrow & & \downarrow \Delta F_4 \\ E(\text{aq}) + MI(\text{aq}) & \xrightarrow{\Delta F_2} & E{:}MI(\text{aq}) \end{array}$$

as well as free-energy simulation methods.

From thermodynamic cycle (3), it follows that

$$\Delta\Delta F = \Delta F_2 - \Delta F_1 = \Delta F_4 - \Delta F_3, \qquad (4)$$

and if the original and the mutated are not too different, the desired quantity can be obtained by the simulation of nonphysical processes 3 and 4. This type of methodology has been used extensively for the prediction and interpretation of protein:ligand interactions as well as in the study of other similar biological processes [35−49].

A very large number of theoretical and experimental studies have been performed to provide a better understanding of the fundamental biological mechanisms associated with the serine proteases. These studies have included quantum and molecu-

lar mechanics calculations [50−52], spectroscopic techniques [53, 54], statistical analysis of crystallographic structures [55, 56], and molecular simulations [57−65]. However, although the binding interactions responsible for the stability of the trypsin−PTI complex have been identified by the analysis of crystallographic structures [66, 67], no systematic study of their relative importance has been carried out.

In this work, we present the study of three different interactions (Asp E189−Lys I15, Gln E192−Cys I14, and Tyr E39−Ile I19) involving side chains from trypsin and PTI (see Fig. 4) and occurring in their contact region (the notation adopted in the remaining text uses $E$ for enzyme and $I$ for inhibitor). These interactions have large differences in their chemical properties and occurring environments. In fact, while Asp E189−Lys I15 is an interaction involving charged side chains, Gln E192−Cys I14 and Tyr E39−Ile I19 are side-chain−main-chain polar interactions. On the other hand, while the first two interactions occur in the hydrophobic binding pocket, the last occurs in a more solvent-accessible hydrophilic region.

In the study of these interactions, we used the indirect pathway described above. The mutations were performed in trypsin, creating a modified trypsin (MTrypsin), and were selected to destroy the specificity of the associated interactions with minor topological alterations. Therefore, our calculations are relative to the first thermodynamic cycle in Eq. (3).

Both thermodynamic perturbation [68] and thermodynamic integration [69] were used in the free-energy simulations performed here. In the thermodynamic perturbation calculations, double-wide sampling [70] was used. In the thermodynamic integration calculations, the free-energy differences, $\Delta F_3$ and $\Delta F_4$, were obtained by trapezoidal integration.

Molecular simulations of biomolecules, in a box of water with periodic boundary conditions, have become possible [41, 43, 46, 71−73]. However, this approach is still too expensive for most of the proteic systems. In this context, the "active region" methododology is a very common alternative [35−40, 43, 44, 46, 61, 63]. Within this formalism, the simulated system is subdivided into an active region (centered in the region of interest) treated by full molecular dynamics or Monte Carlo, a boundary region (where the atomic motions are stochastically [36−38, 40, 43−44] and/or harmonically [35, 36−40, 43, 44, 46, 61, 63] restrained to

**FIGURE 4.** $C_\alpha$-trace representation of the structures of trypsin in green and PTI in red. The binding interactions studied in this work are shown fully: in blue bold, the Gln E192–Cys I14 interactions; in magenta bold, the Tyr E39–Ile I19; and in orange bold, the Asp E189–Lys I15 interactions. For simplicity, the notation *E* for enzyme and *I* for inhibitor has been separated from the names of the residues.

prevent water molecules from evaporation and structural distortions of the amino acid residues near the surface of the model system), and an inert region where the residues are fixed to their initial positions [35, 39, 43, 44, 63] or even deleted [36–38, 40, 46, 61]. Despite its simplicity, this type of method has achieved, in many cases, an agreement between the simulated and the experimental values comparable to the most sophisticated models [74].

Trypsin and the trypsin–PTI complex are relatively large proteic sytems. Consequently, we used an ''active region'' formalism in the molecular dynamics simulations performed in this work. The X-ray diffraction structures of bovine trypsin (resolution = 1.55 Å) and the trypsin:PTI complex (resolution = 1.8 Å) [75d], which include some crystallographic waters, were used as starting geometries in our study. For each interaction, an 18 Å sphere

centered on the mutated amino acid defined the region of interest. The space within this sphere which was not occupied by crystallographically determined atoms was filled by equilibrated TIP3P waters [76]. The model systems used in the simulations are presented in Table II.

The initial structures were fully optimized, until the rms energy gradients were less or equal 0.0001 kcal/mol, using 1000 steps of steepest descent and performing the remaining steps by the conjugate gradients method. In the free-energy simulations, we used 29 windows (0.0025, 0.01–0.05 with increments of 0.01; 0.1–0.9 with increments of 0.05; 0.95–0.99 with increments of 0.01 and 0.9975) for the Tyr E39 $\rightarrow$ Phe mutation [63], and 27 windows (0.01–0.05 with increments of 0.01; 0.1–0.9 with increments of 0.05; 0.95–0.99 with increments of 0.01) for the other two mutations. For each window, molecular dynamics was used to calculate

the ensemble average quantities. The 18 Å spherical region was subdivided into a (15 Å radius) active region treated by full molecular dynamics and a boundary region (with volume between 15 and 18 Å) where harmonic forces were used to restrain the water molecules' motions; this was achieved by constraining the oxygen atoms of these molecules to their starting positions using a force constant of 0.6 kcal mol$^{-1}$ Å$^{-2}$. The other residues were fixed in their initial positions, but were included in the calculation of potential energy and forces. Constant temperature was maintained at 300 K using the Berendsen temperature coupling method [77] with a time step of 0.001 ps and a coupling constant of 0.1 ps. SHAKE constraints [78] were applied to all bonds between hydrogen and heavy atoms. A distance cutoff of 9.0 Å and the SWITCH truncation scheme were used in generating the list of nonbond pairs, updated every 10 steps. Instant values of thermodynamic quantities were kept every 20 steps (0.02 ps) for analysis.

For each window, the ensemble average quantities were equilibrated until their mean values appeared to be stable. In that moment, the production run began and it was continued until the results had converged. The equilibration times ranged from 20 ps to 1 ns and the simulation times from 120 ps to 1.2 ns. All the calculations were performed using an HP/700 workstation, with the package CHARMm© 22 [79], using the standard polar hydrogen potential-energy function linearly scaled with the coupling parameter λ. The free-energy calculations were carried out using the "dual-topology" formalism and the TSM utility. The total simulation times used for each mutation are presented in Table III.

The block methodology [80] with a block size of 100 conformations was used to calculate the statistical errors of the ensemble average quantities. The formalism used to calculate the total errors associated with the free-energy variations ($\Delta F_3$, $\Delta F_4$, and $\Delta\Delta F$) is described elsewhere [63, 81, 82].

The free-energy variations, calculated within the thermodynamic perturbation and thermodynamic integration formalisms, are presented in Table IV. The binding free energies ($\Delta\Delta F$) calculated by both methods are in good agreement. However, their components ($\Delta F_3$, $\Delta F_4$) have usually large discrepancies. The main reason for these differences is that, in thermodynamic integration simulations, the free energies associated with the transitions to the end points were not evaluated. However, if an end-point correction was to be introduced to the thermodynamic integration values (see Table IV), a better agreement could be obtained with the thermodynamic perturbation results.

For each mutation, the individual free-energy components associated with the nonphysical processes ($\Delta F_3$, $\Delta F_4$) are always positive. As expected,

**TABLE II**

**Model systems used in the simulation of specific mutations on trypsin and trypsin–PTI complex.**

| Interaction | Mutation | Center of the 18 Å sphere | Model for solvated trypsin | Model for solvated tripsin–PTI complex |
|---|---|---|---|---|
| Asp E189–Lys I15 (*sc*) | Asp E189 → Ala | $C_\beta$ (Asp E189) | 223 amino acids + 393 TIP3P waters | 281 amino acids + 417 TIP3P waters |
| Tyr E39–Ile I19 (*sc–mc*) | Tyr E39 → Phe | $C_\zeta$ (Tyr E39) | 223 amino acids + 601 TIP3P waters | 281 amino acids + 465 TIP3P waters |
| Gln E192–Cys I14 (*sc–mc*) | Gln E192 → Leu | $C_\gamma$ (Gln E192) | 223 amino acids + 458 TIP3P waters | 281 amino acids + 354 TIP3P waters |

*sc*—side-chain interaction; *sc–mc*—side-chain–main-chain interaction.

**TABLE III**

**Total simulation times used in the simulation of specific mutations on trypsin and trypsin–PTI complex.**

| Interaction | Mutation | Simulation times (ns) | | |
| | | Trypsin | Trypsin–PTI | Total |
| --- | --- | --- | --- | --- |
| Asp E189−Lys I15 (*sc*) | Asp E189 → Ala | 4.560 | 5.760 | 10.320 |
| Tyr E39−Ile I19 (*sc−mc*) | Tyr E39 → Phe | 6.240 | 6.400 | 12.640 |
| Gln E192−Cys I14 (*sc−mc*) | Gln E192 → Leu | 5.520 | 5.880 | 11.400 |

*sc*—side-chain interaction; *sc−mc*—side-chain−main-chain interaction.

a mutation of a specific residue by another destabilizes both trypsin and trypsin−PTI solvated species. This effect is as large as are the differences in chemical properties and topology between the original and mutated residues. In fact, while a large destabilization occurs for the Asp E189 → Ala (charged → nonpolar) mutation, the other two (polar → nonpolar) mutations are significantly less effective. However, Tyr is more similar to Phe than is Gln to Leu, and this explains the smaller destabilization induced by the first mutation relatively to the second.

The binding free-energy values ($\Delta\Delta F$) depend on the associated interactions and on the respective occurring environments. In the association process, a large number of water molecules are removed from trypsin and the PTI species to form the trypsin−PTI complex. The overall stabilization effect of a given ($A, B$) pair depends on the balance between the hydrogen bonds established by residues $A$ and $B$ with the solvent in the initial state [trypsin(aq) + PTI(aq)] and the specific interaction $A−B$ in the trypsin-PTI(aq) complex. The environment where this interaction occurs also has an important role: In a hydrophilic environment, residues $A$ and $B$ can establish a large number of interactions with the solvent and with other polar or charged residues which stabilize the complex.

In this context, Asp E189−Lys I15 is a very strong interaction involving charged side chains, and despite the hydrophobic environment where it occurs, this explains the large positive $\Delta\Delta F$ value

**TABLE IV**

**Calculated free-energy variations (kcal/mol).**

| Interaction | Mutation | Free-energy variation | TP[a] | TI[b] | TI/TP[c] |
| --- | --- | --- | --- | --- | --- |
| Asp E189−Lys I15 (*sc*, **vs**) | Asp E189 → Ala | $\Delta F_4$ | 114.7 ± 0.2 | 115.4 ± 0.2 | 114.4 ± 0.2 |
| | | $\Delta F_3$ | 85.5 ± 0.2 | 87.1 ± 0.1 | 85.2 ± 0.2 |
| | | $\Delta\Delta F$ | 29.2 ± 0.3 | 28.3 ± 0.2 | 29.2 ± 0.3 |
| Tyr E39−Ile I19 (*sc−mc*, **m**) | Tyr E39 → Phe[d] | $\Delta F_4$ | 9.9 ± 0.2 | 11.4 ± 0.1 | 9.4 ± 0.3 |
| | | $\Delta F_3$ | 5.8 ± 0.3 | 7.1 ± 0.1 | 5.1 ± 0.3 |
| | | $\Delta\Delta F$ | 4.1 ± 0.4 | 4.3 ± 0.2 | 4.3 ± 0.4 |
| Gln E192−Cys I14 (*sc−mc*, **w**) | Gln E192 → Leu | $\Delta F_4$ | 39.4 ± 0.3 | 39.5 ± 0.2 | 39.1 ± 0.3 |
| | | $\Delta F_3$ | 51.4 ± 0.3 | 52.0 ± 0.1 | 51.2 ± 0.3 |
| | | $\Delta\Delta F$ | − 12.0 ± 0.4 | − 12.5 ± 0.2 | − 12.1 ± 0.4 |

*sc*—side-chain interaction; *sc−mc*—side-chain−main-chain interaction. **vs**—very strong; **m**—moderate; **w**—weak.
[a] Thermodynamic perturbation.
[b] Thermodynamic integration.
[c] Thermodynamic integration from the first to the last window; thermodynamic perturbation to the end points.
[d] Results from [63].

($\approx 29$ kcal/mol) associated with the Asp E189 → Ala mutation. On the other hand, Tyr E39–Ile I19 and Gln E192–Cys I14 are significantly weaker polar side-chain–main-chain interactions. However, the first interaction occurs in a more hydrophilic region than in the second. Consequently, while the Tyr E39 → Phe mutation is associated with a small positive $\Delta\Delta F$ value ($\approx 4$ kcal/mol), the Gln E192 → Leu mutation is associated with a negative $\Delta\Delta F$ value ($\approx -12$ kcal/mol). The last value is unexpected from a normal point of view. In fact, the Gln E192 → Leu mutation destabilizes the final state in thermodynamic cycle (3) ($\Delta F_4 \approx 39$ kcal/mol), which incorrectly suggests an important binding effect of the Gln E192–Cys I14 interaction. However, the desolvation penalty associated with this mutation is significantly more effective in the destabilization of the final state ($\Delta F_4 \approx 51$ kcal/mol). Consequently, the mentioned interaction probably does not undertake an important role in the formation of the trypsin:PTI complex, because the desolvation penalty in the initial state is not recovered by the hydrogen bonds established in the final state. In the same context, it has been recently suggested that the formation of salt bridges and of hydrogen-bonded neutral pairs is not particularly favored in protein folding [31, 32]. Unfortunately, and at this stage, there are no experimental data to compare the theoretical results with. However, we hope to be able to test these results in the near future.

## Interactions Involved in the Inhibition of Trypsin by PTI

As mentioned before, PTI is a natural inhibitor of trypsin, binding to the active-site region across a tightly packed interface that is crosslinked by a complex network of hydrogen bonds. PTI is a small protein of 58 amino acids. Its native structure is stabilized by three disulfide bridges. The three-dimensional structure consists of a $3_{10}$ helix (N-terminal part), an antiparallel $\beta$-sheet, and an $\alpha$-helix (C-terminal part). Moreover, the portion of PTI in contact with the trypsin active site resembles the bound substrates. In this case, it becomes difficult to explain the reason why no reaction occurs between these two molecules and why they form so stable a complex. The association constant of the complex formed between trypsin and PTI is one of the highest known ($10^{13}$ mol$^{-1}$) [83]. Its

structure has been resolved by X-ray crystallography. The 3D structure used, of 1.8 Å resolution, for the calculations in our study was taken from the Protein Data Bank and its reference is *2ptc* [75d]. Figure 5 represents the Pl site of PTI in the active site of trypsin: the catalytic triad and binding pocket.

The catalytic triad is formed by three amino acids: histidine E57, aspartic acid E102, and serine E195. Lysine I15 (sequence number in the PDB file) of PTI is the Pl site and its side chain is maintained in the S1 site of trypsin by hydrogen bonds between the $NH_3^+$ group and two amino acids: an aspartic acid (E189) and a serine (E190). The presence of at least three water molecules can be noticed, which could play a role in the stability of the complex by forming strong hydrogen bonds with both amino acids of PTI and of trypsin. This complex is very interesting because PTI places a peptidic bond between a lysine (I15) and an alanine (Ala I16) in the catalytic triad of trypsin exactly as a cleavable peptide would do, with the side chain of the lysine in the binding pocket. At this stage, one has to admit that the peptidic bond between Lys I15 and Ala I16 assumes a tetrahedral conformation. However it seems that there is no nucleophilic attack from the serine on this bond and, consequently, no formation of the acylenzyme. As pointed out before, it would be interesting to understand why such a conformation of the active site does not lead to the activation of the enzyme.

Knowing that these interactions are mostly hydrogen bonds, we had to decide on a particular choice of method to perform the necessary calculations. Molecular mechanics force fields are parametrized to reproduce model systems and small departures from them. This renders them inefficient to reproduce reality where active sites of enzymes are concerned. On the other hand, accurate ab initio calculations would have had to be performed only on the active site due to their complexity and associated computing time; this would not have given us the electrostatic influence of the entire complex. However, the fact that PTI is placed in the active site like a cleavable peptide would do and that there is apparently no reaction between PTI and trypsin seems to point to an influence which could be steric or electrostatic. Therefore, performing geometry optimizations only on the active site without the influence of the environment would not have been enough. For all the above-mentioned reasons, a QM/MM method seems very attractive. Recently, a method which
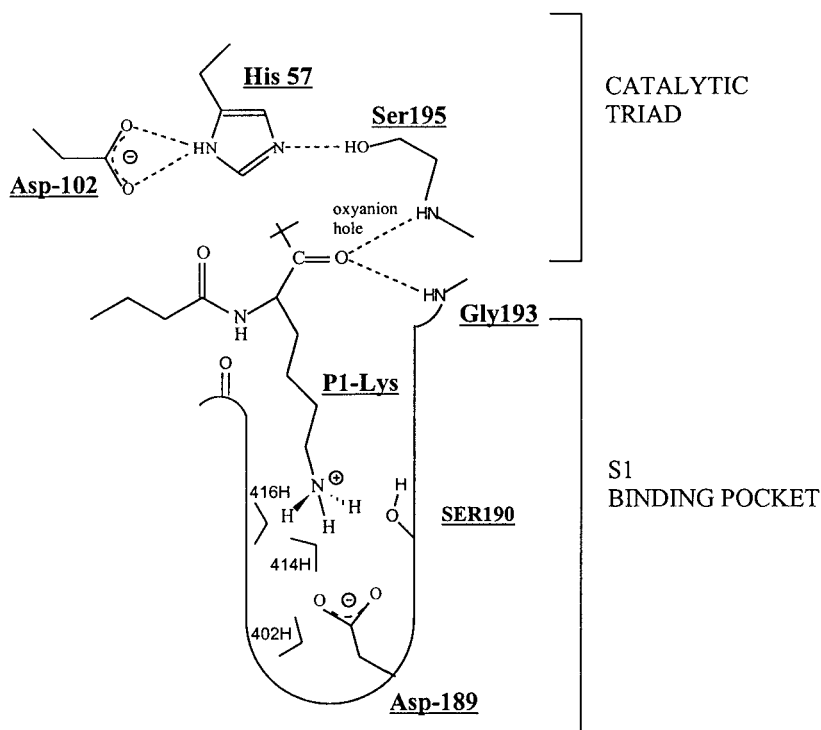
**FIGURE 5.** Binding site of complex trypsin–PTI: P1 site of PTI in the active site of trypsin (catalytic triad and binding pocket). For simplicity, the notation *E* for enzyme and *I* for inhibitor has been separated from the names of the residues.

allows a quantum chemical treatment of a part of a macromolecule mostly described classically has been proposed by some of us under the name of method (LSCF) [7]. This method has been developed at the NDDO semiempirical level. It has been shown that the description of the quantum subsystem is quite comparable to that reached by a whole quantum chemical computation in the systems in which such a computation is possible. We decided to use this method, which allows us to combine a quantum treatment of a small subsystem, the catalytic site and the "substrates," to a classical treatment of the rest of the system. Here, we present QM/MM geometry optimizations of the active site of the complex enzyme–inhibitor.

We first performed molecular mechanics minimizations of the whole system (enzyme, inhibitor, crystallization water molecules, and calcium ion) to which were added counterions (eight sodium, 23 chloride) and two layers of water (the external one being constrained during the minimizations) representing 4018 molecules. Then, we performed QM/MM minimizations of the same system, divided between a quantum subsystem and a classical environment.

The classical minimizations were performed using the Discover© [84] package, with the CVFF [89] force field. A minimized structure, with a gradient less than 0.001, was obtained after 100 steps of steepest descent and more than 7000 steps of conjugate gradient, with a dielectric constant equal to 4.

All our QM/MM calculations were performed using the GEOMOP program in which the LSCF method was implemented a few years ago [7]. The semiempirical method used was AM1 [5], and the force field, CVFF [85], to describe the environment. As we would like to study precisely the conformation of the reactive site involving the catalytic triad and the peptidic bond between Lys I15 and Ala I16 of PTI, our quantum parts involved amino acids His E57, Asp E102, Ser E195, Gly E193, Lys I15, and Ala I16.

Gly E193 and Ser EI95 stabilize the oxyanion hole, that is, the CO group of Lys I15. As the program imposes certain conditions for the choice of frontier atoms, we also included atoms from Ala E56, Cys E58, Ile E103, Asn E101, Gln E192, Asp E194, Gly E196, Cys I14, and Arg I17. The classical environment was constituted by all other atoms of

the PDB file. Figure 6 shows all the atoms included in the quantum part.

The optimized geometry of the active site is shown in Figure 7 in which interesting interactions are characterized by dashed lines between atoms. We focused on seven interactions—potential hydrogen bonds—labeled $i1$ to $i7$. Corresponding distances and angles are reported in Table V, in which we also show geometric values from the PDB structure.

If we call $A$ the acceptor atom and $D$ the donor atom ($A$----$H$-$D$), we can describe a hydrogen bond by three parameters: distance $d$, which is the distance between $A$ and the hydrogen atom of $hb_1$; $d'$, representing the distance between $A$ and $D$; and $\theta$, the angle (AHD). The distances $d'$ are
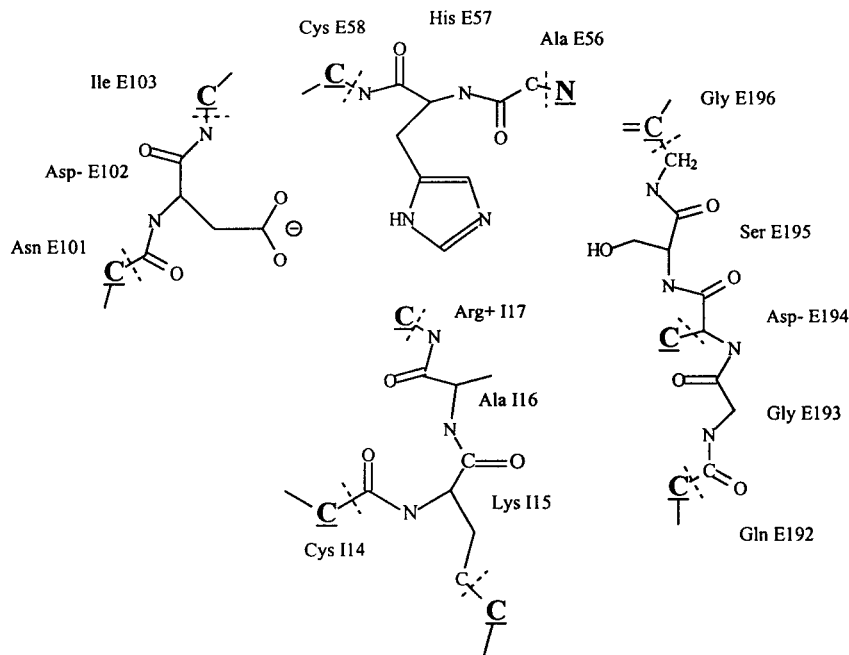


**FIGURE 6.** Atoms included in the quantum part of the QM/MM calculations. Bold underlined characters are used for MM frontier atoms. Dashed lines represent the frontiers.
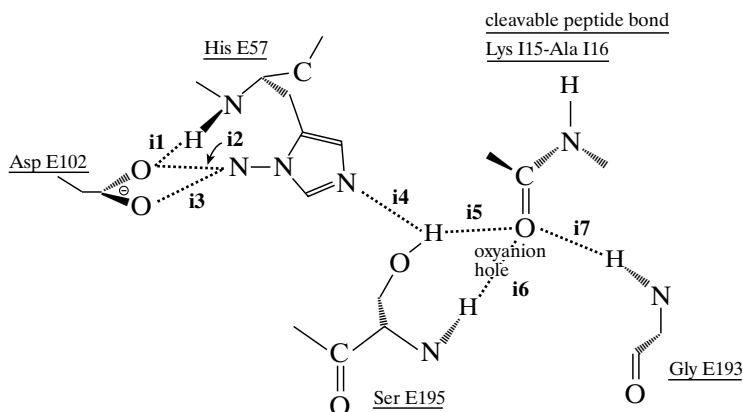


**FIGURE 7.** Interactions between amino acids of the active site in the complex trypsin-PTI. Corresponding distances and angles have been reported in Table V.

**TABLE V**
**Result of QM/MM mlnimizations; distances and angles.**

| | | crystallographic data [4d] | QM/MM minimized structure |
|---|---|---|---|
| i1 | $d_1$ (Å) | — | 2.2 |
| | $d'_1$ (Å) | **3.1** | **3.2** |
| | $\theta_1$ (°) | — | 157.6 |
| i2 | $d_2$ | — | 2.1 |
| | $d'_2$ | **3.2** | **3.1** |
| | $\theta_2$ | — | 168.7 |
| i3 | $d_3$ | — | 2.3 |
| | $d'_3$ | **2.6** | **3.0** |
| | $\theta_3$ | — | 128.7 |
| i4 | $d_4$ (Å) | — | 3.9 |
| | $d'_4$ (Å) | **2.6** | **3.3** |
| | $\theta_4$ (°) | — | 42.5 |
| i5 | $d_5$ | — | 2.1 |
| | $d'_5$ | **3.04** | **2.9** |
| | $\theta_5$ | — | 136.7 |
| | (COH) | — | 95.2 |
| | ($C^\beta O^\gamma N_{His\ E57}$) | **103.2** | **79.8** |
| | $d(O^\gamma_{Ser\ E195} - C_{Lys\ I15})$ | 2.68 | 3.2 |
| i6 | $d_6$ | — | 2.4 |
| | $d'_6$ | **2.8** | **3.1** |
| | $\theta_6$ | — | 134.7 |
| | (COH) | — | 155.5 |
| i7 | $d_7$ | — | 2.4 |
| | $d'_7$ | **2.8** | **3.2** |
| | $\theta_7$ | — | 136.3 |
| | (COH) | — | 93.9 |

necessary to compare the results of the calculations to the crystallographic data, because of the absence of the hydrogen atoms' positions in the X-ray structures.

The carboxylate group (Asp E102) is hydrogen-bonded to His E57 as was found in the X-ray structure. We found at least two hydrogen bonds: The first one is formed by $O^{\delta 1}$ and the nitrogen atom of His E57 and the second lies between the same oxygen atom and $N^\delta$ of the same histidine. In both structures, for each of these interactions, the distance between the acceptor atom ($O^{\delta 1}$) and the hydrogen atom linked to the donor ($N^\delta$ or $\dot{N}$) is smaller than the sum of the van der Waals radii of hydrogen and oxygen atoms (2.7 Å). Moreover,

$\theta$ angles have values from 158° to 175°, significant of the existence of hydrogen bonds. Especially for i2, the values of the $d$ distances and the $\theta$ angles described above show that this hydrogen bond is a strong one. Moreover, the distances $d'_2$ (3.1 and 3 Å) obtained after the calculation are in good agreement with crystallographic data (3.2 Å). There seems to be another hydrogen bond (interaction i3), probably weak, between the $O^{\delta 2}$ of aspartate and the $N^\delta$ of the imidazole ring. Indeed, we found a distance of 2.3 Å between the acceptor and the hydrogen atom and values of 128.7° for $\theta$.

The value found for the $O^\gamma_{Ser\ E195} - N^\varepsilon_{His\ E57}$ distance is 3.3 Å (interaction i4). This value is bigger than the PDB value (2.6 Å) but not too far from the same distance in nonliganded trypsin [75d]. This structure does not exhibit the presence of a strong hydrogen bond between serine and histidine. On the contrary, it seems that the hydroxyl group of the serine is hydrogen-bonded to the carboxyl group of the Lys I15, P1 site of PTI (interaction i5). As found in the PDB structure, the nitrogen atoms of Gly E193 and Ser E195 are hydrogen-bonded to the carboxyl group of lysine, the oxyanion hole.

From our calculations, we found that there is no hydrogen bond between the serine and the histidine of the active site of trypsin in the complex between PTI and trypsin. We can assume that this is the reason why there is no nucleophilic attack of the hydroxyl oxygen on the peptide bond of PTI. However, these calculations are only a preliminary work and this structure might be a local minimum. We must now consider the dynamics of this complex. From the analysis of a 1 ns classical dynamics of the complex [86], we saw that this crucial hydrogen bond exists only half of the time of the simulation. We are now performing the same simulation of the trypsin liganded by a cleavable peptide for comparison and the next step will be a QM/MM dynamic simulation, allowing the accurate treatment of the active site.

## Conclusions

We are interested in the study of enzyme−inhibitor interactions to be able to understand the biology of such processes. Ultimately, we hope to be capable of modeling this type of interaction in relation to enzyme−inhibitor complexes as to predict new inhibitors for trypsinlike serine proteases.

The studies on the complex enzyme–inhibitor have given us useful information concerning the arginine–carboxylate interactions taking place in the binding pocket of β-factor XIIa when in the presence of an inhibitor. Additionally, the calculations of the free energy associated with mutations in the solvated contact region of the complex do give us a clear idea of the contribution of each individual interaction to its stability. The results obtained enable us to conclude that the larger the charge separation of the involved residues and the hydrophilicity of the environment, the larger those contributions are. Finally, the hybrid quantum mechanical–classical mechanical calculations are invaluable in allowing us understand the reasons why PTI is an inhibitor of trypsin rather than a substrate. We hope to have a completely clear picture of every interaction by the time all the calculations are completely done.

In summary, the work that we have presented here is ongoing research which will provide us with useful information on the trypsin–PTI interactions as well as to help us to extrapolate that knowledge to similar processes concerning β-factor XIIa, in particular, and trypsinlike serine proteases, in general.

### ACKNOWLEDGMENTS

# References

1. Stroud, R. M. Sci Am 1974, 231, 74.

2. Kraut, J. Annu Rev Biochem 1977, 46, 331.

3. Vincent, J. P.; Lazdunski, M. Biochemistry 1972, 11, 2967.

4. Hehre, W. J.; Radom, L.; Schleyer, P. v. R.; Pople, J. A. Ab Initio Molecular Orbital Theory; Wiley: New York, 1986.

5. Dewar, M. J. S.; Zoebisch, E. G.; Heale, F.; Stewart, J. J. P. J Am Chem Soc 1985, 107, 3902.

6. Mezei, M.; Beveridge, D. L. Ann NY Acad Sci 1986, 482, 1.

7. Thery, V.; Rinaldi, D.; Rivail, J. L.; Maigret, B.; Ferenczy, G. G. J Comp Chem 1994, 15, 269.

8. Barlow, D. J.; Thornton, J. M. J Mol Biol 1983, 168, 867.

9. Singh, J.; Thornton, J. M.; Snarey, M.; Campbell, S. F. FEBS Lett 1987, 224, 161.

10. Scharnagl, C.; Hettenkofer, J.; Fisher, S. F. J Phys Chem 1995, 99, 7787.

11. Honig, B.; Ottolenghi, M.; Steves, M. Isr J Chem 1995, 35, 429.

12. Lanyi, J. K. Biophys J 1995, 56, 143.

13. Scharnagl, C.; Fisher, S. F. Chem Phys 1996, 212, 231.

14. Dickopf, S.; Heyn, M. P. Biophys J 1997, 73, 3171.

15. Sheriff, S.; Silverton, E. W.; Padlan, E. A.; Cohen, G. H.; Smith-Gill, S. J. Proc Natl Acad Sci USA 1987, 84, 8075.

16. Magalhães, A. L.; Maigret, B.; Hoplack, J.; Gomes, J. A. N. F.; Scheraga, H. A. J Protein Chem 1994, 13, 195.

17. McDonald, S. M.; Wilson, R. C.; McCammon, J. A. Protein Eng 1995, 8, 915.

18. Sreedharan, S. K.; Veerna, C.; Cases, L. S. D.; Brocklehurst, S. M.; Garbia, S. E.; Shah, H. N.; Brocklehurst, K. Biochem J 1996, 316, 777.

19. Kim, D. H.; Park, J. I. Biorg Med Chem Lett 1996, 6, 2967.

20. Wynn, R.; Laskowski, M., Jr. Biochem Biophys Res Commun 1990, 166, 1406.

21. Görbitz, C. H. Acta Crystallogr B 1989, 45, 390.

22. Ippolito, J. A.; Alexander, R. S.; Christianson, D. W. J Mol Biol 1990, 215, 457.

23. Mitchell, J. B. O.; Thornton, J. M.; Singh, J. J Mol Biol 1992, 226, 251.

24. Sapse, A. M.; Russell, C. S. Int J Quantum Chem 1984, 26, 91.

25. Sapse, A. M.; Russell, C. S. J Mol Struct (Theochem) 1986, 137, 43.

26. Mitchell, J. B. O.; Nandi, C. L.; Thornton, J. M.; Price, S. L.; Singh, J.; Snarey, M. J Chem Soc Faraday Trans 1993, 89, 2619.

27. Melo, A.; Ramos, M. J. Chem Phys Lett 1995, 245, 498.

28. Melo, A.; Ramos, M. J.; Floriano, W. B.; Gomes, J. A. N. F.; Leão, J. F. R.; Magalhães, A. L.; Maigret, B.; Nascimento, M. C.; Reuter, N. J Mol Struct (Theochem), accepted for publication.

29. Melo, A.; Ramos, M. J. Int J Quantum Chem, accepted for publication.

30. Zheng, Y.-J.; Ornstein, R. L. J Am Chem Soc 1996, 118, 11237.

31. Hendsch, Z. S.; Sindelar, C. V.; Tidor, B. J Phys Chem 1998, 102, 4404.

32. Barril, X.; Aleman, C.; Orozco, M.; Luque, F. L. Proteins Struct Funct Genet 1998, 32, 67.

33. Frisch, M. J.; Trucks, G. W.; Head-Gordon, M.; Gill, P. M. W.; Wong, M. W.; Foresman, J. B.; Johnson, B. G.; Schlegel, H. B.; Robb, M. A.; Replogle, E. S.; Gomperts, R.; Andres, J. L.; Raghavachari, K.; Binkley, J. S.; Gonzalez, C.; Martin, R. L.; Fox, D. J.; Defrees, D. J.; Baker, J.; Stewart, J. J. P.; Pople, J. A. Gaussian 92, Revision A; Gaussian, Inc.: Pittsburgh, PA, 1992.

34. Davies, G. J.; Mackenzie, L.; Varrot, A.; Dauter, M.; Brzozowski, A. M.; Schulein, M.; Withers, S. G. Biochemistry 1998, 37, 11707.

35. Menziani, M. C.; Reynolds, C. A.; Richards, W. G. J Chem Soc Chem Commun 1989, 853.

36. Gao, J.; Kuczera, K.; Tidor, B.; Karplus, M. Science 1989, 244, 1069.

37. Tidor, B.; Karplus, M. Biochemistry 1991, 30, 3217.

38. Simonson, T.; Brünger, A. T. Biochemistry 1992, 31, 8661.

39. Zacharias, M.; Straatsma, T. P.; McCammon, J. A.; Qiocho, F. A. Biochemistry 1993, 32, 7428.

40. Lau, F. T. K.; Karplus, M. J Mol Biol 1994, 236, 1049.

41. Pearlman, D. A.; Connelly, P. R. J Mol Biol 1995, 248, 696.

42. Brady, G. P.; Sharp, K. A. J Mol Biol 1995, 254, 77.

43. Liang, G.; Schmidt, R. K.; Yu, H. A.; Cumming, D. A.; Brady, J. W. J Phys Chem 1996, 100, 2528.

44. Simonson, T.; Archontis, G.; Karplus, M. J Phys Chem B 1997, 101, 8349.

45. Gilson, J. K.; Given, J. A.; Bush, B. L.; McCammon, J. A. Biophys J 1997, 72, 1047.

46. Fox, T.; Scanlan, T. S.; Kollman, P. A. J Am Chem Soc 1997, 119, 11571.

47. Veenstra, D. L.; Kollman, P. A. Protein Eng 1997, 10, 789.

48. Archontis, G.; Simonson, T.; Moras, D.; Karplus, M. J Mol Biol 1998, 275, 823.

49. Hermone, A.; Kuczera, K. Biochemistry 1998, 37, 2843.

50. Deggett, V.; Shroder, S.; Kollman, P. A. J Am Chem Soc 1991, 113, 8926.

51. Bencsura, A.; Enyedy, I.; Kovach, M. Biochemistry 1995, 34, 8989.

52. Dive, G.; Dehareng, D.; Peeters, D. Int J Quantum Chem 1996, 58, 85.

53. Frey, P. A.; Whitt, S. A.; Tobin, J. B. Science 1994, 264, 1927.

54. Ash, E. L.; Sudmeier, J. L.; Defalo, E. C.; Bachovchin, W. W. Science 1997, 278, 5340.

55. Hubbard, S. J.; Thornton, J. M.; Campbell, S. F. Faraday Discuss 1992, 93, 13.

56. Perona, J. J.; Craig, C. S. Protein Sci 1995, 4, 337.

57. Heiner, A. P.; Berendsen, H. J. C.; van Gunsteren, W. F. Protein Eng 1993, 6, 397.

58. Miyamoto, S.; Kollman, P. A. Proc Natl Acad Sci USA 1993, 90, 8402.

59. Åqvist, J. J Comp Chem 1996, 17, 1587.

60. Joneshertzog, D. K.; Jorgensen, W. L. J Med Chem 1997, 40, 1539.

61. Essex, J. W.; Severance, D. L.; Tirado-Rives, J.; Jorgensen, W. L. J Phys Chem B 1997, 101, 9663.

62. Resat, H.; Marrone, T. J.; McCammon, J. A. Biophys J 1997, 72, 522.

63. Melo, A.; Ramos, M. J. J Peptide Res 1997, 50, 382.

64. Guo, Z. Y.; Brooks, C. L. J Am Chem Soc 1998, 120, 1920.

65. Bentzien, J.; Muller, R. P.; Florian, J.; Warshel, A. J Phys Chem B 1998, 102, 2293.

66. Janin, J.; Chothia, C. J Mol Biol 1976, 100, 197.

67. Bode, W.; Schwager, P.; Huber, R. Miami Winter Symp 1976, 11, 43.

68. Zwanzig, R. W. J Chem Phys 1954, 22, 1420.

69. Kirkwood, J. G. J Chem Phys 1935, 3, 300.

70. Jorgensen, W. L.; Ravimohan, C. J Chem Phys 1985, 83, 3050.

71. Yan, Y.; Erickson, B. W.; Tropsha, A. J Am Chem Soc 1995, 117, 7592.

72. Norberg, J.; Nilsson, L. J Am Chem Soc 1995, 117, 10832.

73. Guo, Z.; Brooks, C. L., III; Kong, X. J Phys Chem B 1998, 102, 2032.

74. Fox, T.; Kollman, P. A. Proteins Struct Funct Genet 1996, 25, 315.

75. (a) Rühlmann, A.; Kukla, D.; Schwager, P.; Bartels, K.; Huber, R. J Mol Biol 1973, 77, 417. (b) Stroud, R. M.; Kay, L. M.; Dickerson, R. E. J Mol Biol 1974, 83, 185. (c) Huber, R.; Kukla, D.; Bode, W.; Schwager, P.; Bartels, K.; Deisenhofer, J.; Steigemann, W. J Mol Biol 1974, 89, 73. (d) Marquart, M.; Walter, J.; Deisenhofer, J.; Bode, W.; Huber, R. Acta Crystallographica B 1983, 39, 480.

76. Jorgensen, W. L.; Chandrasekhar, J.; Madura, J.; Impey, R. W.; Klein, M. L. J Chem Phys 1983, 79, 926.

77. Berendsen, H. J. C.; Postma, J. P. M.; van Gunsteren, W. F.; DiNola, A.; Haak, J. R. J Chem Phys 1984, 81, 3684.

78. Ryckaert, J. P.; Ciccoti, G.; Berendsen, H. J. C. J Comp Phys 1977, 23, 327.

79. Brooks, B. R.; Bruccoleri, R. E.; Olafson, B. D.; States, D.; Swaminanthan, S.; Karplus, M. J Comp Chem 1983, 4, 187.

80. Gao, J.; Berne, B. J. J Chem Phys 1989, 91, 6359.

81. Pearlman, D. A. J Chem Phys 1993, 98, 8946.

82. Pearlman, D. A. J Comp Chem 1994, 15, 105.

83. Voet, D.; Voet, J. G. Biochemistry; Wiley-International: New York, 1995.

84. Discover; Molecular Simulations Inc.: San Diego, CA, 1997.

85. Dauber-Osguthorpe, P.; Roberts, V. A.; Osguthorpe, D. J.; Wolff, J.; Genest, M.; Hagler, A. T. Proteins 1988, 4, 31.

85. Unpublished results, work in progress.